

Honors Thesis

COMPUTATIONAL DEVELOPMENT OF A MINIATURE QUANTUM DOT
SPECTROMETER FOR USE IN SPACE

By

Joseph Gabriel Richardson

Submitted to Brigham Young University in partial fulfillment of graduation requirements for
University Honors

Department of Physics and Astronomy

Brigham Young University

April 21, 2021

Advisor: Dr. David Allred, BYU

Advisor: Dr. Mahmooda Sultana, NASA GSFC

Honors Coordinator: Dr. Steven Turley

ABSTRACT

COMPUTATIONAL DEVELOPMENT OF A MINIATURE QUANTUM DOT SPECTROMETER FOR USE IN SPACE

Joseph Gabriel Richardson

Department of Physics and Astronomy

Bachelor of Science

Miniature spectrometers are of great interest to NASA as necessary instrumentation is scaled down and optimized for specific space applications. Semiconductor nanocrystals called quantum dots (QD) are being used to create a miniature high-resolution filter-based spectrometer, with the goal of use in space within five years. Computational imaging techniques—such as automated image analysis and mathematical spectrum reconstruction algorithms—are two of the key aspects to making the QD spectrometer a reality. This thesis discusses the process of developing these computational methods, along with the improvements that have occurred from previous work.

Keywords: Quantum Dot, Spectrometer, NASA, Computational Imaging, Ill posed inverse problem, image analysis, SciKit Image, reconstruction, Python, MATLAB

Acknowledgments

This project would not have been possible without the amazing mentorship of Dr. David Allred and Dr. Mahmooda Sultana. I am also grateful for the mentorship of Dr. Manuel Quijada and Javier Del Hoyo in the Optics branch at NASA Goddard Space Flight Center and Dr. Steven Turley at Brigham Young University. Of course, I would like to thank my family and my amazing wife Marissa who have listened to my babbling thoughts, a process that has been key for my understanding.

Table of Contents

Table of Contents	vii
List of Figures	ix
1 Introduction	1
1.1 <i>Background</i>	1
1.2 <i>Motivation</i>	2
2 Methods	4
2.1 <i>Physical Setup</i>	4
2.2 <i>Computational Setup</i>	6
3 Results and Conclusions	10
3.1 <i>Image Analysis and Pixel Mapping</i>	10
3.2 <i>Mathematical Spectrum Reconstruction</i>	14
3.3 <i>Discussion of Results</i>	19
Index	20
References	21

List of Figures

Figure 1	The process by which a quantum dot spectrometer operates.	5
Figure 2	QDS architecture, showing spectrometer pixels overlaying CCD pixels.....	7
Figure 3	On the top, the quantum dot filter used for initial development.....	8
Figure 4	From left to right: The high contrast image of a simple quantum dot filter array.....	11
Figure 5	From left to right: Original CCD image vs. post use of inverse Gaussian algorithm. ..	12
Figure 6	Image of sorted dot groups after detection	13
Figure 7	From left to right: Plot of original dot, plot of detected pixels, and an overlay.	13
Figure 8	A plot of the 3 sample spectra available for development of the reconstruction	14
Figure 9	Plot of the root means square error (RMSE) for the 3 samples with high noise.	16
Figure 10	Plot of the root means square error (RMSE) for the 3 samples with medium noise. ..	17
Figure 11	Plot of the root means square error (RMSE) for the 3 samples with low noise.	18

1 Introduction

1.1 Background

Quantum Dots (QD) are semiconductor nanocrystals, ranging in size from two to 20 nm, with novel optical properties.¹ Various applications of QDs have been considered since at least the late 1990's², and they are currently being researched for a wide range of applications, from renewable energy to high resolution displays.³

The focus of this thesis is the development of computational methods that make the QD spectrometer a reality. Although these methods are discussed in the context of the quantum dot spectrometer, they can be applied to other instances where reconstruction occurs.

With an extensive body of understanding on quantum dots, MIT researchers from the Bawendi group were the first to use the unique filtering properties of QDs to create a novel miniature spectrometer.⁴ A QD filter with known absorption and transmission properties is placed in front of a detector. The detector converts the incoming signal, post filters, into

computationally usable data. A reconstruction algorithm uses known filter data along with the detected signal to obtain the original spectrum.

Since the release of the Bawendi findings in 2015, further research has been performed that builds upon the initial prototype. For example, other filtering methods and reconstruction methods have been tested.^{5 6 7 8 9} A multispectral imager using quantum dot spectrometer is currently under development by the Sultana group at NASA's Goddard Space Flight Center, in collaboration with the Bawendi group, for future space applications. The research presented in this thesis was performed as a part of the team at NASA Goddard.

1.2 Motivation

The primary motivation for creating a QD spectrometer is the ability to miniaturize spectral and hyper-spectral imaging instrumentation. Spectrometers are important instruments for understanding the physical world¹⁰ and are used widely by NASA to understand our Earth and other celestial bodies.^{11 12}

The quantum dot spectrometer would not function without the use of computational methods. Two primary computational methods have been developed to enable the QD spectrometer. First, the pixel mapping and image analysis program enables accurate use of QD spectrometer pixels. Second, the mathematical spectrum reconstruction algorithm returns the original spectrum using filter property data, data obtained by the CCD, and data from the pixel mapping algorithm. This process will be further explained in Chapter 2.

Reconstruction algorithms are common to many other computational imaging processes, for example CT scans and other medical imaging.^{13 14 15} The basic idea is that it is necessary to obtain an unknown incoming signal using know variables and properties. Some of the techniques researched in this thesis were developed for use in medical imaging applications and were modified for spectrum reconstruction.

2 Methods

This chapter contains information regarding the physical and computational mechanisms that make the quantum dot spectrometer a reality. To understand the importance of the computational algorithms that were developed for this thesis, it is important to understand what role they play in conjunction with the hardware of the quantum dot spectrometer. Prototype creation method are discussed, as well as the data that was available for computational development.

2.1 Physical Setup

The quantum dot spectrometer requires both hardware and software elements to function (see Fig. 1 for a graphic of how this process works). Although this thesis is primarily focused on the software components, to understand the computational setup it is necessary to understand the physical setup. The quantum dot spectrometer is composed of two primary physical components. First, an array of quantum dot filters (here referred to as spectrometer pixels because of their

purpose in modifying the spectrum, like a normal spectrometer), and second a charged coupled device (CCD).

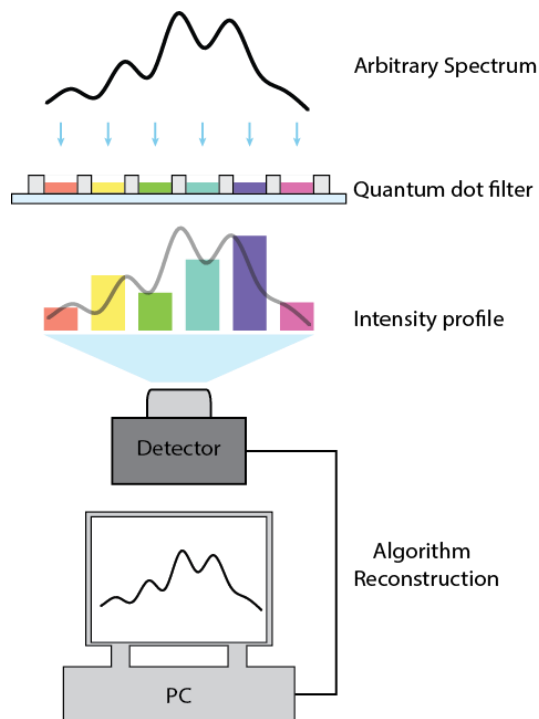


Fig. 1 The process by which a quantum dot spectrometer operates.

The optical properties of quantum dots have a uniquely tunable nature. These semiconductor nanocrystals, varying in size between one and twenty nm, will absorb light at different wavelengths depending on their size and composition. This is largely due to the quantum dot being smaller than twice the Bohr radius of the bulk exciton.¹⁶ An advanced process has been developed for quantum dot creation and optical parameter tuning which is proprietary to our collaborators in the Bawendi group.

To create an array of quantum dot pixels, a suspension of quantum dots is deposited as a localized thin film. Once the solvent evaporates, we are left with a solid pixel made of only

quantum dots. Various methods for creating the spectrometer pixel array are being investigated and optimized by Dr. Sultana's group at NASA GSFC.

With the ability to create quantum dot arrays, a basic instrument testbed was developed. A monochromatic light source shines through the quantum dot array, and data is obtained through the CCD. A LabView program is used for instrument operation and data collection. The data from the CCD is then used for spectral reconstruction, as explained in the following section.

2.2 Computational Setup

Spectrum reconstruction is the process for obtaining the original spectrum computationally. In the prototype phase, this is accomplished using data from the instrument testbed. The simplified idea of spectrum reconstruction is solving what is considered an ill posed inverse problem. The basic structure of an ill posed inverse problem is:

$$Ax = b + e$$

where matrix A represent previously obtained characteristic transmission data for each of the quantum dot filter, vector b is the data obtained from the CCD after light passes through the filter array, and vector e is the error that results from various factors. Vector x is the original spectrum of light, which is what we wish to obtain. A and b are known while x and e are unknown, leading to the ill posed nature of the inverse problem. This equation does not describe the exact nature of the error present in the system, and in chapter 3 experimentation related to understanding systematic error will be described.

Two types of data are provided by the instrument testbed. The first is an image of the quantum dot spectrometer pixel filter array, and the second is the raw filtered data obtained by

the CCD (vector $b + e$). The image of the filter array is important as data from the CCD must be matched to the previously obtained transmission data of each quantum dot spectrometer pixel (see Fig. 2). The image analysis algorithm matches the location of individual CCD pixels to the corresponding spectrometer pixels. This process allows the spectral reconstruction algorithm to match which transmission data corresponds to which filter, essentially putting the matrix in the correct order.

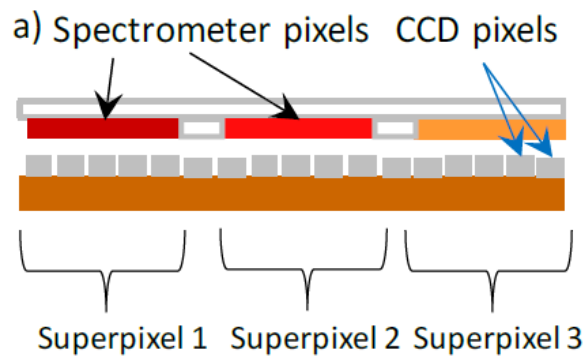


Fig. 2 QDS architecture, showing spectrometer pixels overlaying CCD pixels, together forming super pixels.

For initial development of the image analysis program, a clear image of the quantum dot filter array was obtained using a high-resolution microscope. This clear image has a uniform background which provided a high contrast between the spectrometer pixels and the background (See Fig. 3). The high contrast made development of the image analysis algorithm much easier. Once the image analysis algorithm was performing well with the clear image, a process for analyzing a raw CCD image from the instrument testbed was developed.

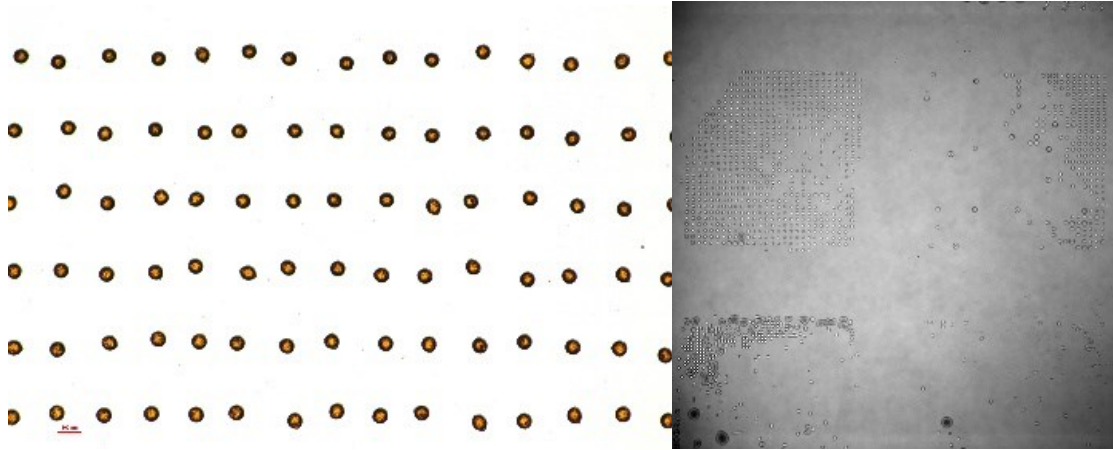


Fig. 3 On the left, the quantum dot filter used for initial development. On the right, the filter captured by the CCD.

Scikit image (an open-source library in Python popular for image analysis) was used to develop the image analysis algorithm. Various techniques were employed to perform the image segmentation. The final technique will be explained in chapter 3.

For spectrum reconstruction, open-source MATLAB algorithms were investigated and tested. The benefit of using open-source algorithms (either through MATLAB or online) is predominantly in saving time. Not having to create algorithms from scratch, but instead adapting existing algorithms allowed for more algorithms to be tested. There were 14 different reconstruction algorithms that were researched and tested, including: least squares non-negative (MATLAB `lsqnonneg`), Tikhonov regularization, expectation-maximization algorithm, Convex Optimization Toolbox (Stanford University), total variation augmented lagrangian (TVAL3), Global Optimization Pattern Search package (MATLAB), function minimization constrained (MATLAB `fmincon`), sparse sensing, total variation denoise, L1 Magic, linear least squares (MATLAB `lsqlin`), function minimization unconstrained (MATLAB `fminunc`), genetic algorithm (MATLAB Global Optimization Toolbox), particle swarm (MATLAB Global Optimization Toolbox).

Of the 14 tested, six algorithms performed the most accurate reconstructions of the original spectra. These six algorithms perform differently depending on the circumstance, such as amount of noise and spectral structure playing a factor in reconstruction accuracy. The precise details of performance will be explained in Chapter 3.

3 Results and Conclusions

This chapter covers the results and analyses of the pixel mapping program and the spectrum reconstruction algorithms. Discussions of performance in the presence of error are presented, and conclusions are drawn.

3.1 Image Analysis and Pixel Mapping

As explained in chapter 2, two images were used to develop the pixel mapping algorithm. The technique developed to achieve successful image segmentation was mostly a result of trial and error, but basic principles were established to yield best results. For the first image with a high contrast between the dots and the background (see Fig. 4), the following process was developed:

Step 1: Convert image to gray scale. Scikit image has functions that will do this automatically.

Step 2: Segmentation. To achieve segmentation, three Scikit image functions were used.

- 1. Thresholding. During this process, individual pixels are categorized either as foreground or background. Both Otsu and Median thresholding was used subsequently to obtain optimal results
- 2. The image is converted to a binary image, where each group of pixels is grouped together as a segment. This is essentially where the segmentation occurs.
- 3. The Scikit image “remove small” algorithm is used to get rid of any small object that are found in the image which are not actually quantum dot filters. The small objects are likely dust.

Step 3: Measure. The Scikit image measure function groups the segmented image into arrays, and the properties of these arrays can now be output. For example, the area the dots are now known.

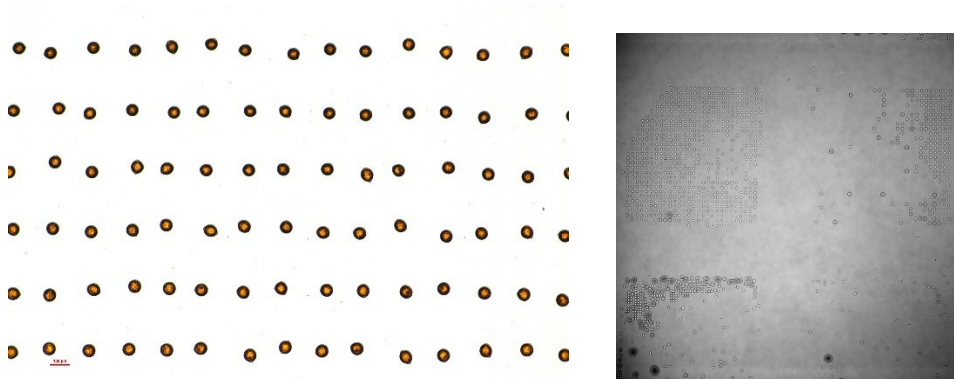


Fig. 4 From left to right: The high contrast image of a simple quantum dot filter array vs. a low contrast image from the CCD.

Segmentation for the image captured by the CCD was slightly different because of the nonuniformity in contrast (see Fig. 4). This nonuniformity caused the process previously developed to not work, as the segmentation algorithm began detecting the dark gradient edges as

dots. A simple solution was eventually discovered. After step 1, an inverse Gaussian algorithm (available within SciKit image) is used. This removes the nonuniformity in the background, creating a much easier image to analyze (see Fig. 5).

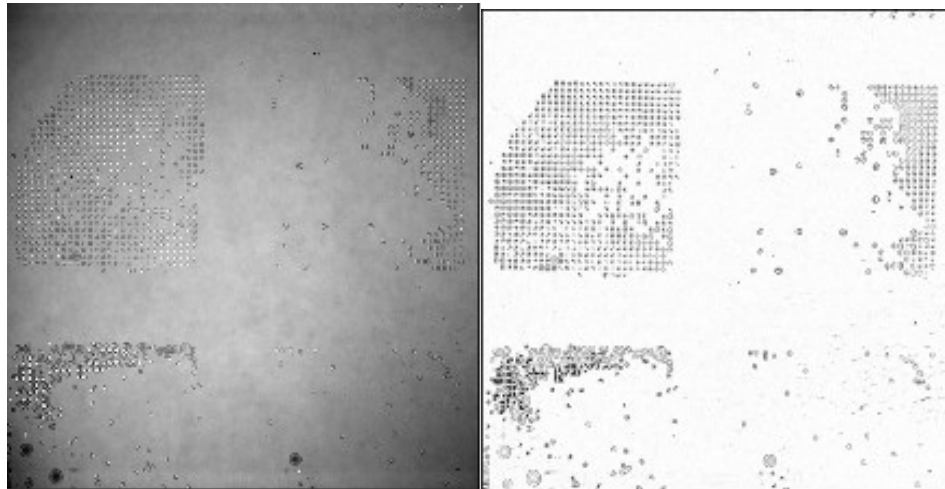


Fig. 5 From left to right: Original CCD image vs. post use of inverse Gaussian algorithm.

Once segmentation is achieved, the program outputs a nested array containing the location of each pixel for each dot, as well as a labeled image of the dot array. Initially, the output of dot location was random (see Fig. 6), but an algorithm was developed to sort the array of dots. This sorted array of pixel locations is important for the function of the Mathematical spectrum reconstruction algorithm.

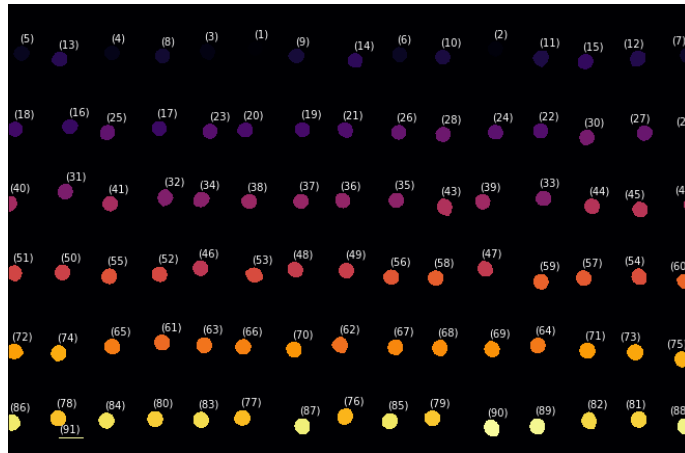


Fig. 6 Image of sorted dot groups after detection

To determine the amount of error present in dot detection, I simply looked at whether the dots we expected to be detected were detected. I also zoomed in on individual dots and compared an overlay of the detected dots and the original image. As can be seen in Fig. 7, the detection is not perfect, and generally overestimates by about 2 pixels around the perimeter of the dot.

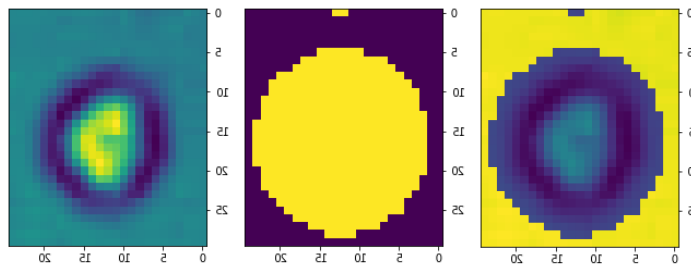


Fig. 7 From left to right: Plot of original dot, plot of detected pixels, and an overlay for comparison of error.

Because there are several parameters that can be changed to improve image segmentation depending on the image contrast, a basic GUI was developed in python for user operation during prototype development. This will likely not have a use in the final version of the quantum dot spectrometer as image quality is standardized but will be useful during prototype development.

The image analysis is performed in python, but the mathematical spectrum reconstruction is performed in MATLAB. It was necessary to develop a protocol for the Python program to

automatically run within MATLAB, and then for the output data to be used in MATLAB. This goal was achieved successfully but has not yet been tested within the context of the prototype testbed.

3.2 Mathematical Spectrum Reconstruction

The mathematical spectrum reconstruction was tested using three sets of data (see Fig. 8). The main difference between these sets of data is the location of the central peak, along with a slight variation in the shape of the peak.

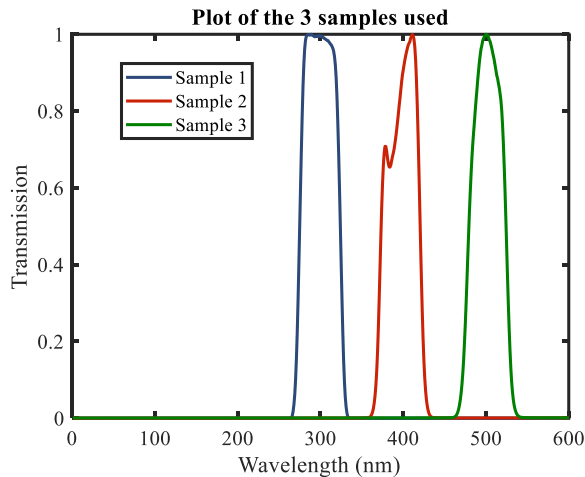


Fig. 8 A plot of the 3 sample spectra available for development of the reconstruction algorithm

As mentioned previously, the reconstruction algorithm was developed in MATLAB. One of the main concerns is to determine how well the reconstruction occurs when performing under varying amounts of error. This error could pretty much come from any component on the spectrometer, or even due to the environment in which the measurement is being taken (IE low light). To preliminarily test performance under error, artificial error was added to the 3 sets of data in 3 different ways:

1. FP: Random uniform noise is added to the matrix of filter data A ($A' = A + rn$)
2. OA: Random uniform noise is added to the vector of detected data b ($b' = b + rn$)
3. OD: Random uniform noise is divided into the vector b ($b' = b/(1+rn)$)

Each of the three ways were tested with three levels of error: High noise ($rn = 10^{-1}$), Medium noise ($rn = 10^{-3}$), and low noise ($rn = 10^{-5}$). The six algorithms that performed best were run each of these 27 ways and compared to one another to determine which algorithm performs the best under various noise constraints (see Fig. 9, 10, and 11). The six best performing algorithms whose results are shown are:

- Lsq = Least Squares (MATLAB lsqnonneg) with Tikhonov Regularization
- Cvx = Convex Optimization (Stanford University Convex Optimizaiton toolbox) with Tikhonov Regularization
- Gauss = Gaussian Learning
- L1 lsq = L1 minimization with least squares (L1 magic package)
- Gauss Cvx = Using gaussian learning followed by convex optimization
- ART = Expectation-Maximization Algorithm (ART toolbox)

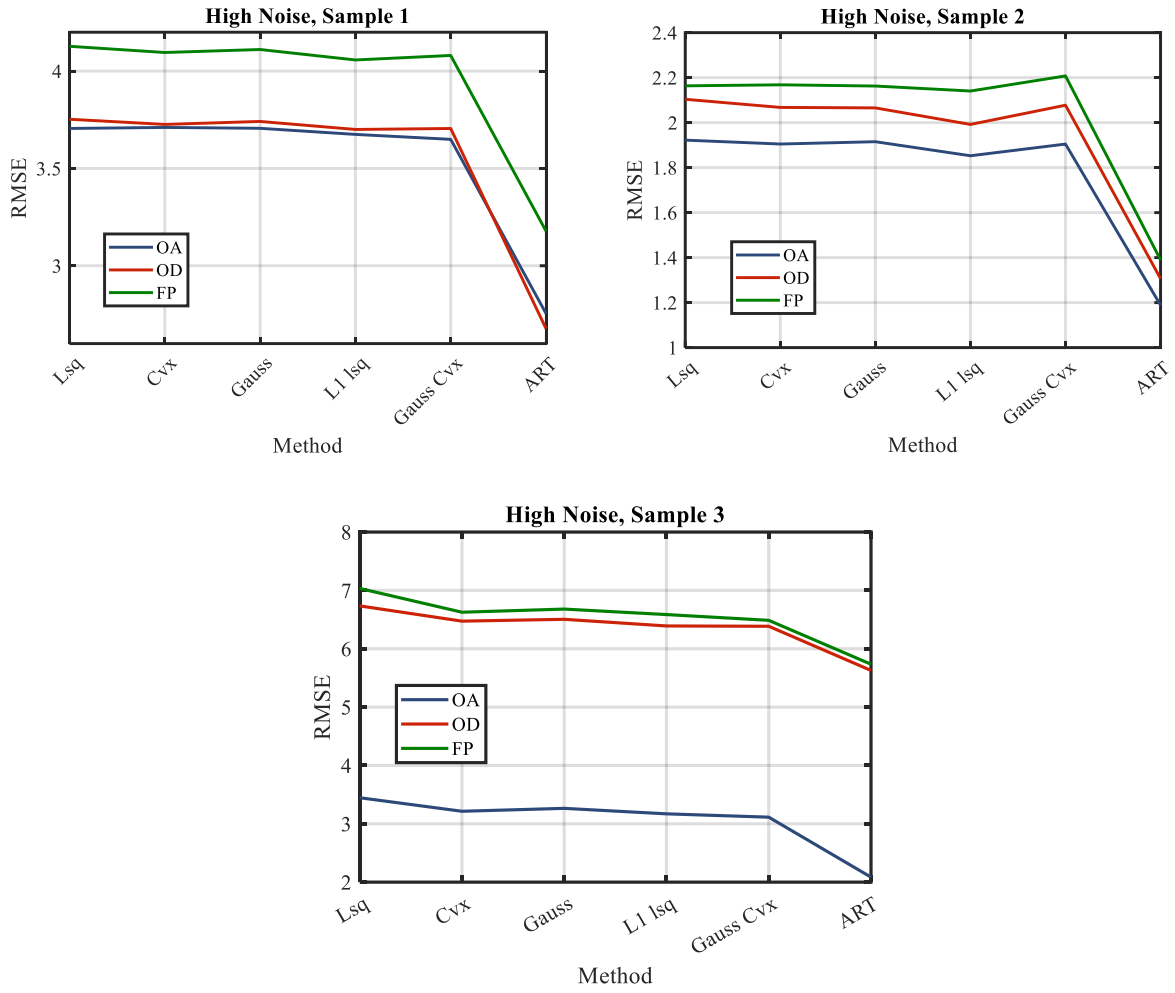


Fig. 9 Plot of the root means square error (RMSE) for the 3 samples with high artificial noise.

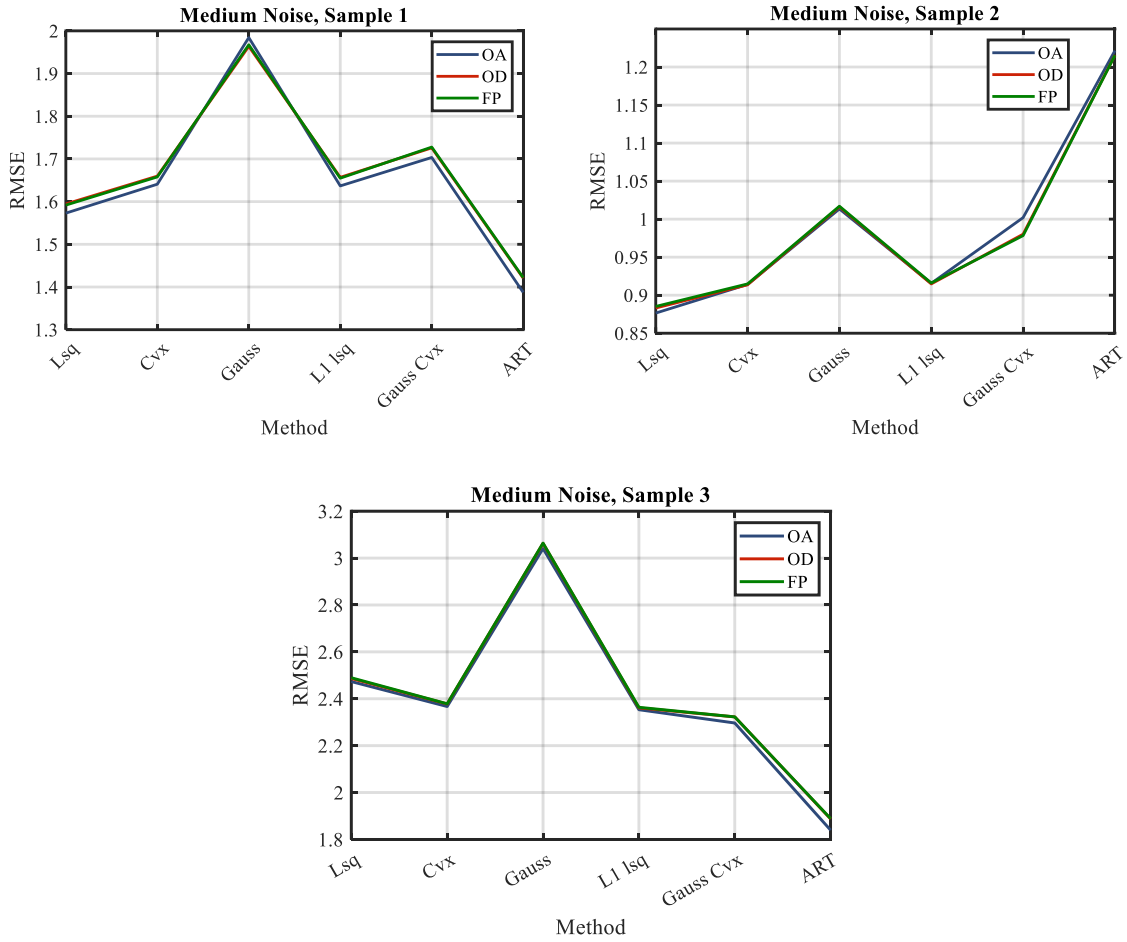


Fig. 10 Plot of the root means square error (RMSE) for the 3 samples with medium artificial noise.

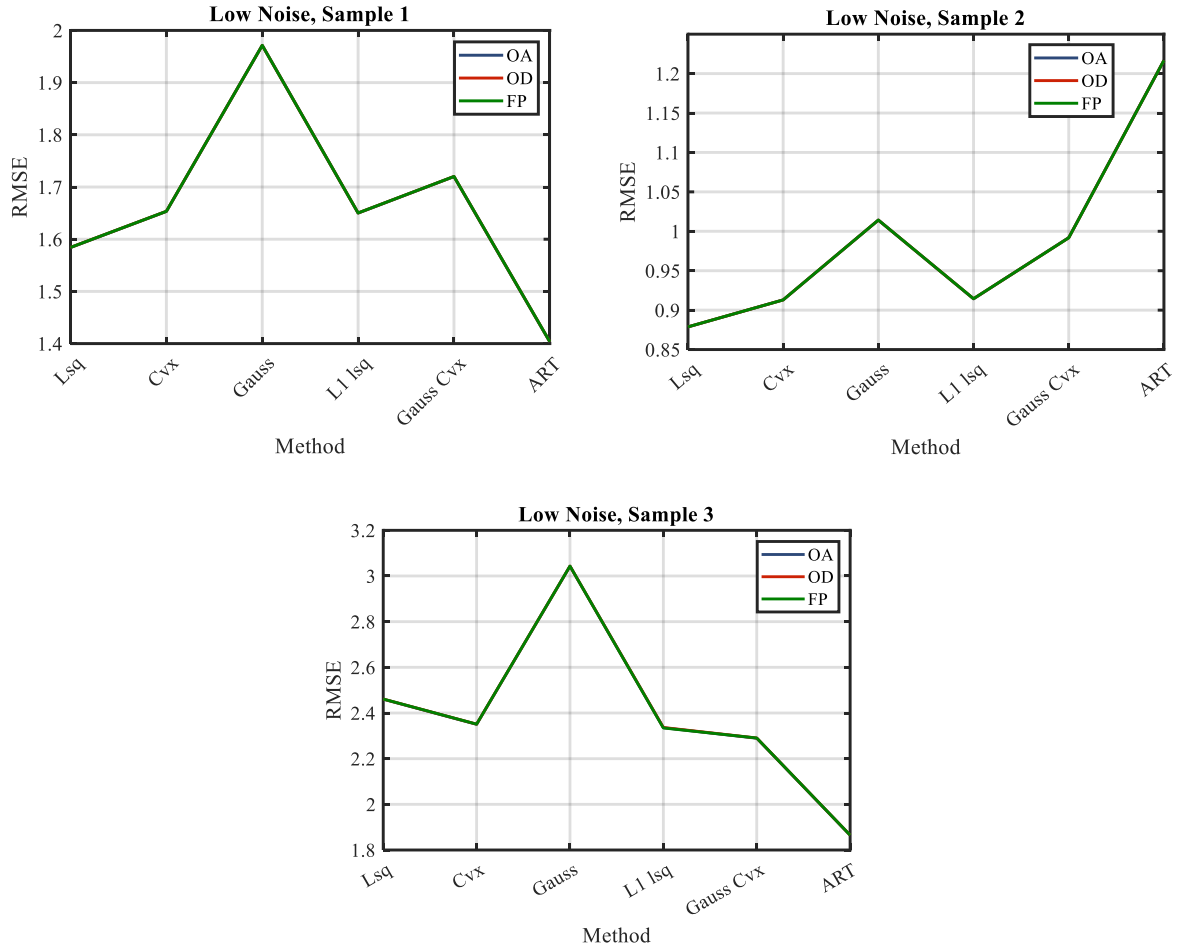


Fig. 11 Plot of the root means square error (RMSE) for the 3 samples with low artificial noise.

We found quickly that different algorithms performed better or worse depending on the sample. From the results, we see that in almost every case the ART algorithm performed the best. The ART algorithm is especially robust under high artificial noise. The only cases where the ART algorithm did not perform the best were under medium and low artificial noise for sample 2. Because each of the samples had a slightly different structure, it appears that the structure of the spectra has a large influence on the performance of the reconstruction algorithm. We can also see that as the noise level gets lower, the different methods of considering noise

become less and less important. At high noise there is a large variation in the performance of the algorithms depending on which method was used to integrate error.

3.3 Discussion of Results

In conclusion, an effective program was developed to successfully analyze images produced by the quantum dot spectrometer. This program was developed for use with both high and low contrast images and with a large degree of accuracy. As prototype development continues for the instrument it will be necessary to modify some of the existing parameters to perform optimally under different conditions, but these parameters are mostly found in the segmentation portion of the algorithms.

Great improvements were also made on the previous state of the art (which is least squares with Tikhonov regularization) for spectrum reconstruction of a quantum dot spectrometer. We found 6 algorithms that achieve best reconstruction overall, and each of the algorithms performs differently depending on the composition of the spectra which is being reconstructed. In the future it appears that the best results might be obtained using a combination of these algorithms. The ART algorithm performs best overall and under the greatest variety of situations, including under instances where high amounts of artificial noise are present.

The Quantum Dot spectrometer is an exciting invention that has the possibility of greatly influencing what can be observed both in space and on Earth. With a miniature, high resolution spectral imager there is the possibility of more frequent observation because weight is no longer a concern. These imaging systems can fit in small satellites called CubeSats, or even carried portably by astronauts as they explore the surface of celestial bodies. Hopefully, the developments explained previously will assist in making these possibilities a reality.

Index

A

Algorithm, 7, 14

ART, 14, 17, 18

E

Expectation-Maximization, 7, 14

I

Image Analysis, v, 2, 9

inverse problem, iii, 6

M

MATLAB, iii, 7, 12, 13, 14

N

NASA, i, iii, iv, 2, 5, 13

noise, vi, 8, 14, 17, 18

P

Python, iii, 7, 12

Q

Quantum Dot, i, iii, 4, 18

Quantum Dot spectrometer, 4, 18

R

reconstruction, iii, vi, i, 2, 3, 5, 6, 7, 9, 11, 12, 13, 17, 18

S

spectrum, iii, i, 3, 6, 7, 9, 11, 12, 18

super pixel, 5, 6

T

Tikhonov regularization, 18

References

- ¹ C.B. Murray, C.R. Kagan, and M.G. Bawendi, *Annu. Rev. Mater. Sci.* **30**, 545 (2000), <https://doi.org/10.1146/annurev.matsci.30.1.545>
- ² Z.I. Alferov, The history and future of semiconductor heterostructures. *Semiconductors* **32**, 1–14 (1998). <https://doi.org/10.1134/1.1187350>
- ³ M.A. Cotta, *ACS Appl. Nano Mater.* **3**, 4920 (2020). <https://doi.org/10.1021/acsanm.0c01386>
- ⁴ J. Bao and M.G. Bawendi, *Nature* **523**, 67 (2015). <https://doi.org/10.1038/nature14576>
- ⁵ X. Zhu, L. Bian, H. Fu, L. Wang, B. Zou, Q. Dai, J. Zhang, and H. Zhong, *Light: Science & Applications* **9**, 73 (2020). <https://doi.org/10.1038/s41377-020-0301-4>
- ⁶ J. Oliver, W. Lee, S. Park, and H.-N. Lee, *Opt. Express*, OE 20, 2613 (2012). <https://doi.org/10.1364/OE.20.002613>
- ⁷ T. Sarwar, S. Cheekati, K. Chung, and P.-C. Ku, *Appl. Phys. Lett.* **116**, 081103 (2020). <https://doi.org/10.1063/1.5143114>
- ⁸ F. Sun, L. Xia, Z. Yang, J. Cui, Z. Zhang, C. Nie, D. Liu, S. Yin, G. Zheng, P. Wu, R. Yang, and C. Du, *IEEE Photonics Journal* **8**, 1 (2016). [doi: 10.1109/JPHOT.2016.2597190](https://doi.org/10.1109/JPHOT.2016.2597190).
- ⁹ Z. Wang, S. Yi, A. Chen, M. Zhou, T.S. Luk, A. James, J. Nogan, W. Ross, G. Joe, A. Shahsafi, K.X. Wang, M.A. Kats, and Z. Yu, *Nature Communications* **10**, 1020 (2019). <https://doi.org/10.1038/s41467-019-08994-5>
- ¹⁰ C.P. Bacon, Y. Mattley, and R. DeFrece, *Review of Scientific Instruments* **75**, 1 (2003). <https://doi.org/10.1063/1.1633025>
- ¹¹ https://spinoff.nasa.gov/Spinoff2010/hm_4.html, Accessed February 10, 2021
- ¹² D. Guzzi, G. Coluccia, D. Labate, C. Latri, E. Magli, V. Nardino, L. Palombi, I. Pippi, D. Coltuc, A.Z. Marchi, and V. Raimondi, in *International Conference on Space Optics — ICSSO 2018* (International Society for Optics and Photonics, 2019), p. 111806B. <https://doi.org/10.1117/12.2536146>
- ¹³ J. Sun, T. Yu, J. Liu, X. Duan, D. Hu, Y. Liu, and Y. Peng, *BMC Medical Imaging* **17**, 24 (2017). <https://doi.org/10.1186/s12880-017-0177-9>
- ¹⁴ E. Kang, J. Min, and J.C. Ye, *Med Phys* **44**, e360 (2017). <https://doi.org/10.1002/mp.12344>
- ¹⁵ K. Lange and R. Carson, *J Comput Assist Tomogr* **8**, 306 (1984). <https://pubmed.ncbi.nlm.nih.gov/6608535/>
- ¹⁶ C.B. Murray, C.R. Kagan, and M.G. Bawendi, *Annu. Rev. Mater. Sci.* **30**, 545 (2000). <https://doi.org/10.1146/annurev.matsci.30.1.545>